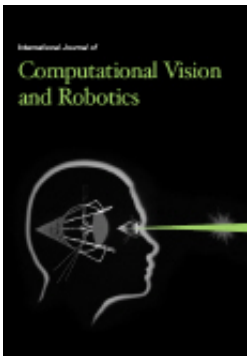

International Journal of Computational Vision and Robotics

ISSN online: 1752-914X - ISSN print: 1752-9131
https://www.inderscience.com/ijcvr

A modified Coye algorithm for retinal vessel segmentation

Sakambhari Mahapatra, Uma Ranjan Jena, Sonali Dash, S. Agrawal

DOI: 10.1504/IJCVR.2022.10044507

Article History:

Received:	29 December 2020
Accepted:	16 December 2021
Published online:	30 November 2022

A modified Coye algorithm for retinal vessel segmentation

Sakambhari Mahapatra and
Uma Ranjan Jena

Department of Electronics and Telecommunication Engineering,
VSS University of Technology,
Burla, India
Email: mahapatra.shakambhari@gmail.com
Email: urjena@rediffmail.com

Sonali Dash

Department of Electronics and Communication Engineering,
Raghu Institute of Technology,
Vishakhapatnum, India
Email: sonali.isan@gmail.com

S. Agrawal*

Department of Electronics and Telecommunication Engineering,
VSS University of Technology,
Burla, India
Email: agrawals.72@gmail.com
*Corresponding author

Abstract: According to a scientific study, eyes are the best predictors of numerous disorders including glaucoma, diabetic retinopathy, hypertension, and stroke. An ophthalmologist can learn about the problems by looking at the segmented retinal blood vessel network. The goal of this study is to offer ophthalmologists with reliable segmented retinal blood vessels to help them pinpoint the issue. This work put forwards an automated method of vessel extraction by incorporating curvelet-based enhancement with the Coye algorithm. Further, the segmentation performance is fine-tuned by embodying a pair of complementary gamma functions (PCGF) for contrast improvement. The suggested approach is evaluated on DRIVE and STARE databases and shows outstanding results as compared to state-of-the-art algorithms.

Keywords: curvelet transform; Coye algorithm; gamma transform; pair of complementary gamma function; PCGF; vessel segmentation.

Reference to this paper should be made as follows: Mahapatra, S., Jena, U.R., Dash, S. and Agrawal, S. (2023) 'A modified Coye algorithm for retinal vessel segmentation', *Int. J. Computational Vision and Robotics*, Vol. 13, No. 1, pp.73–90.

Biographical notes: Sakambhari Mahapatra received her BTech in Electronics and Communication Engineering from BPUT, Odisha in 2010. She received her MTech in Communication System Engineering from VSS University of Technology, Burla. She is working as an Assistant Professor in the Department of Electronics and Telecommunication Engineering, VSS University of Technology, Burla. She has experience in teaching for more than eight years. Her research interest includes biomedical image processing and artificial intelligence.

Uma Ranjan Jena received his BSc in Engineering in 1983 from Sambalpur University, Odisha, India, MTech in 1997 from IIT Kharagpur, India, and PhD in 2003 from Jadavpur University, Kolkata, India. He is working as a Professor in the Department of Electronics and Telecommunication Engineering, VSS University of Technology, Burla. His research interests include computer vision, image processing, and soft computing. He has teaching experience of more than 28 years and has a number of both national and international journals and conferences publications.

Sonali Dash received her BTech in Electronics and Telecommunication Engineering from Utkal University, Odisha, India in 1992. She received her MTech in Electrical Engineering from KIIT Bhubaneswar, Odisha, India in 2005 and PhD in Engineering from VSS University of Technology, Burla. She is working as an Associate Professor in the Department of Electronics and Communication Engineering at Raghu Institute of Technology, Vishakhapatnam, India. She has experience in teaching and industry of more than 18 years. Her research interests include image processing, signal processing, and pattern recognition. She has published many national/international journals and conference papers.

S. Agrawal received his BE and MTech in Electronics and Telecommunication Engineering from UCE Burla, India in 1995 and 2003, respectively, and PhD (Engineering) degree from Sambalpur University, Sambalpur, India in 2015. He is currently an Associate Professor with the Department of Electronics and Telecommunication Engineering, VSS University of Technology, Burla. He has over 50 papers in International Journals and Conferences. He has over 800 Google Scholar citations with an h-index of 14. His current research interests include digital signal/image processing, biomedical engineering, and soft computing. He is a member of ISTE and IEEE.

1 Introduction

The retina is the only part of the human body that allows direct non-invasive visualisation of its anatomical structures. Several large-scale population-based surveys reported statistical correlations between structural variation in retina's vascular system with various diseases like hypertension, stroke, and cardiovascular disorder (Khan et al., 2019a). For example, presence of a tiny capillary near the small vessels is an early sign of DR. Similarly, proliferative DR is marked by unusual proliferation of new blood vessels. The temporal change of retinal vessel width and tortuosity give an indication of retinopathy of prematurity. The ratio of arteries to veins width is associated with hypertension and cardiovascular disorder. The examination of such retinal microvasculature necessitates the use of precise technologies to extract the vascular tree

in order to quantify the morphological changes and assess the patients' status. Furthermore, the retinal vascular tree has been discovered to be unique to each person and can be utilised for biometric identification also. Although, manual annotation of vessels is possible, it is time-consuming, tedious, and prone to human error when carried out in large numbers. It also requires training and skill. Hence, automatic vessel extraction is needed. But the incorporation of noise, variation in image intensity, and poor image contrast, etc. put substantial difficulties for the reliability of vessel annotation. Furthermore, the shape, size, and grey level of blood vessels can all be very different, and some background elements may have similar characteristics as vessels. Vessel crossing/branching and loss of vessel connectivity due to poor illumination and contrast can further complicate the annotation process.

Many researchers have recommended different methods for extracting the vasular network from the fundus image. These methods are broadly classified as:

1 unsupervised methods like thresholding approach, clustering approach, tracking methods, etc.

2 supervised methods such as support vector machine (SVM), artificial neural network-based classification (Moccia et al., 2018).

In most of these approaches, image enhancement is a pre-requisite step that helps in removing the noise, making the background homogeneous, and improving the contrast between the vessel and the non-vessel regions. It also tries to highlight the edges and fine details of the vessels. These image enhancements can be carried out in the spatial domain i.e., modifying directly the pixel intensity values like GC, histogram, equalisation, morphological operations or it may be done in the transform domain, i.e., discrete wavelet transform (DWT), Gabor transform, curvelet transform (CT), etc. Enhancement can also be done by combing these methods. Dash et al. (2020) combined contrast limited adaptive histogram equalisation (CLAHE) and GC for image quality improvement, and successively applied Gabor and Hessian transforms to enhance the fundus image. It is learnt that the gamma intensity correction is very frequently applied on the retinal image for contrast improvement. Dash and Bhoi (2017) put forwarded an adaptive thresholding technique on gamma-corrected retinal images for vasculature extraction. Piecewise GC followed by histogram equalisation is suggested by Reddy et al. (2018) for fundus image enhancement. Khan et al. (2019b) applied a scale-normalised second-order Gaussian derivative detector on contrast-enhanced fundus image and flood-filled reconstruction strategy to get the binary image. Sreejini and Govindan (2015) implemented a multiscale Gaussian matched filter for the said purpose.

Koh et al. (2017) estimated various DWT features for classifying several diseases in the retinal image. Dash and Senapati (2020) decomposed the retinal image through various wavelets and applied Tyler Coye algorithm (Coye, 2015) to trace the vessel network. DWT in integration with match filtering is adapted by Wang et al. (2013) for de-noising and enhancing the fundus image. The vessels are further extracted through adaptive thresholding. Roychowdhury et al. (2015) implemented Gaussian mixture model that utilised pixel-based features, first and second-order gradients for classifying vessel and non-vessel pixels. Mapayi et al. (2015) suggested a local adaptive thresholding technique based on the gray level cooccurrence matrix for vessel delineation. Pal et al. (2019) applied morphological gray level hit-or-miss transform for better segmentation performance. Memari et al. (2019) applied genetic algorithm-based fuzzy C-means

clustering to trace the initial blood vessel layout and further fine-tuned the result by an integrated level set approach. Zhou et al. (2020) traced the major structures of the vessel using an improved line detector and the thin vessels were detected using the Hidden Markov model. Ricci and Perfetti (2007) suggested the SVM that takes line detector response as a feature vector. The Gabor filter in combination with the Bayesian classifier is also suggested by Soares et al. (2006) for vessel enhancement. Yadav (2020) suggested the ridglet transform and histogram equalisation for fundus figure quality improvement and artificial neural network to classify normal and abnormal cases. The CT was first analysed by Starck et al. (2003) for image enhancement purposes.

The curvelet can better represent the lines, edges, and curvatures in all the directions compared to the other multi-resolution techniques. This ability has been explored by many researchers for fundus image de-noising and enhancement. Kar and Maity (2016) proposed CT and match filtering for enhancement and intensification of the retinal vasculature. Following this, they applied fuzzy c-means clustering to get the vessel network. CT with length filtering is suggested by Miri et al. (2010) for vessel extraction in the retinal image. Strisciuglio et al. (2016) investigated the B-COSFIRE filters for vessel enhancement. Coye (2015) put forwarded a simple and straight forward algorithm for retinal vessel extraction. Bandara and Giragama (2017) integrated various enhancement techniques and hough line transformation-based vessel reconstruction approach with a variant of Tyler Coye algorithm, for extracting retinal vessels. But, they ended up with a lower segmentation Accuracy (Acc).

In the original Tyle Coye algorithm, although the contrast between the background and vessels is enhanced before segmentation, the vessel edges and curvatures are not intensified. Furthermore, it is quite evident that incorporating a suitable technique for highlighting the vessel edges and contours can improve the segmentation results. This has motivated us to incorporate the curvelet-based vessel enhancement along with pair of complementary gamma function (PCGF) in the Coye algorithm for the problem on hand. Here, we suggest a novel modification to the original Tyler Coye algorithm by incorporating the curvelet-based vessel enhancement and de-noising. The CT is implemented to enhance the vessels and de-noise the image. The curvelet coefficients are modified in a very simple manner. The inverse CT with the modified set of coefficients give the enhanced image where the vessel edges and curvatures are sharpened and intensified effectively. Moreover, in the proposed approach, the PCGF has been incorporated to take care of the illumination variation and improve the overall contrast of the retinal image. Finally, the vessel network is extracted using ISODATA thresholding. The experiments are conducted with two standard fundus databases. The outcomes are compared with state-of-the-art published work on retinal vessel segmentation. It is observed that our proposed method give high quality segmented vessel structures as compared to other methods.

The main contributions of this work are:

1 A new amendment to Coye algorithm for retinal vessel extraction is suggested.

2 A simple curvelet coefficient modification approach is investigated for vessel edge and curvature enhancement.

3 PCGF based contrast enhancement for the retinal image is examined.

4 The evaluated results are compared with state-of-the-art methods.

The remaining part of the paper is arranged as follows. Section 2 gives a brief explanation of the materials and methods used in the work. The suggested approach is discussed in detail in Section 3. Section 4 discusses the results and performance of the suggested approach and Section 5 concludes the paper.

2 Materials and methods

The basic analysis of the techniques that contribute to the proposed approach is presented in this section.

2.1 Pair of complementary gamma function

The gamma correction (GC) is a spatial domain operation, which modifies each pixel intensity of the input image by γ times (Gonzalez et al., 2004). This function increases the brightness of the image throughout due to which the bright areas become brighter resulting in poor image visibility. So, Li et al. (2020) proposed a new pair of gamma correction function (PCGF) that can delicately balance the brightness and contrast of the image in both the dark and the bright regions. Here, the enhanced image y is the weighted summation of the two mapped images y_1 and y_2, which are also estimated from the original input image x by the following way.

$$y = w_1 y_1 + w_2 y_2 \tag{1}$$

Here y_1 and y_2 are computed as below:

$$y_1 = 1 - (1 - x)^{\gamma} \tag{2}$$

$$y_2 = \left(1 - (1 - x)^{1/\gamma}\right)^{\gamma} \tag{3}$$

The weight factors w_1 and w_2 are determined as

$$w_1 = \frac{\overline{y_1}}{\overline{y_1} + \overline{y_2}} \qquad w_2 = \frac{\overline{y_2}}{\overline{y_1} + \overline{y_2}} \tag{4}$$

Here $\overline{y_1}$ and $\overline{y_2}$ are the average intensity values of the mapped images y_1 and y_2. Since the weight factors are directly related to the mean intensity values, so the equivalent mapping in the output image will have a moderate brightness. Equation (2) and (3) shows a complementary relationship and by integration of these two equations, a moderate exposed and high quality image can be achieved. As PCGF achieves a delicate balance between the underexposure and the overexposure areas, it can effectively boost the contrast of the dark and the bright regions in the image at the same time.

2.2 Curvelet Transform

The CT was first proposed by Donoho and Duncan (2000). It was designed with the objective of representing edges and other singularities along curves more effectively than typical wavelet transforms and other members of that family. It is a multiscale transform,

with the elements indexed by level s and orientation parameters θ. The digital CT applied on a 2D image $f(m, n)$, gives a set of curvelet coefficients $C(s, \theta, k_1, k_2)$ as

$$C(s,\theta,k_1,k_2) = \sum_{\substack{0<m<M \\ 0<n<N}} f(m,n)\ \varphi_{s,\theta,k_1,k_2}[m,n] \tag{5}$$

Here M and N are the horizontal and vertical dimensions of the image respectively. k_1 and k_2 are the spatial location of the curvelet φ. For implementing the curvelet transform, first a 2D FFT of the image is computed. The 2D frequency plane is divided into concentric squares representing different levels of decomposition. Then radial partitions are done to the frequency plane that correlates to angular orientations θ. Each segment that results because of the partition of the frequency plane to concentric squares and radial division, is termed as a wedge. Hence, each wedge is specified by level s and the orientation θ. These wedges catch the edges, curvatures, and singularities in various directions, which make the CT highly anisotropic and directional sensitive. Finally, an inverse FFT of each wedge is calculated to collect the curvelet coefficients in the spatial domain for each s and θ. These coefficients in each level represent different frequency regions of the image. The coefficients for level s = 1 represent the low-frequency region of the image. Similarly, the coefficients in the higher decomposition levels carry details of the high-frequency regions. These coefficients are modified in a specific manner to highlight certain regions in the image. The resultant image is reconstructed using the modified curvelet coefficients through inverse curvelet transform.

2.3 Tyler Coye algorithm

In 2015, Coye put forwarded a new methodology for retinal vasculature extraction in the fundus image. Here instead of the green channel, they utilised the gray image. The gray image is obtained from the RGB fundus image through principal component analysis (PCA). The first stage in this grey image conversion is the production of vector colour images, which is generated by stacking three colour channels. Then, using the traditional transfer function, a zero-mean *YCbCr* image is computed to separate the luminance and chrominance channels. In the next step, the eigenvalues of each component are determined and PCA is used to obtain the associated eigenvectors. A linear combination of three projections produces the final grey image with weights determined by their eigenvalues. The contrast of the gray image is then adjusted via CLAHE. Successively the background exclusion is done by deducting the mean filtered image from the enhanced image. Finally, the vessel annotation is achieved via ISODATA thresholding.

3 Proposed method

The suggested approach investigated a new modification to the original Coye algorithm by incorporating the curvelet based vessel enhancement strategy. The schematic overview of the suggested approach is presented in Figure 1.

Figure 1 Schematic overview of the proposed approach

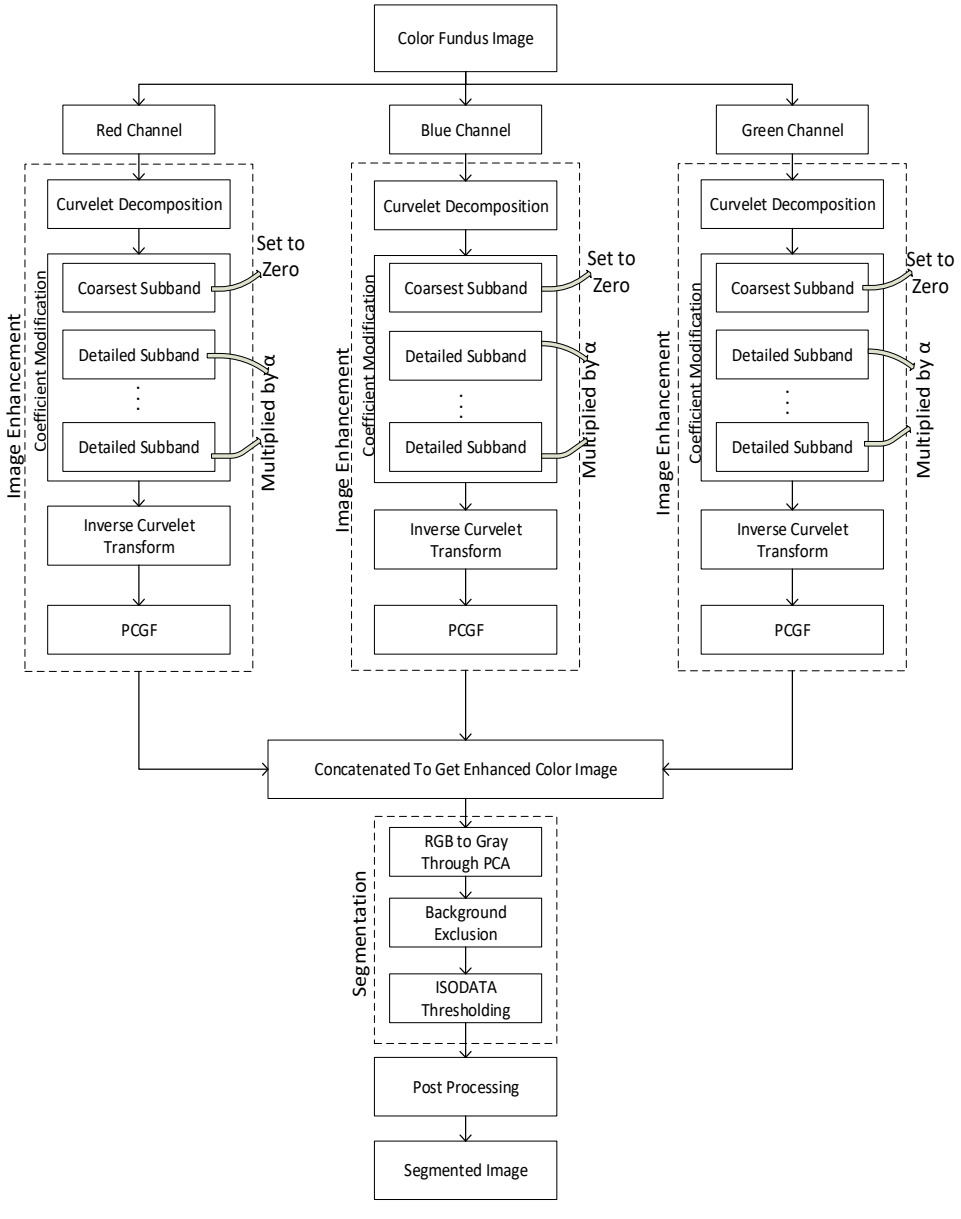

The Coye algorithm utilised a gray image generated from the RGB in place of the green channel alone. Therefore, in the suggested approach, each channel is enhanced separately in order to preserve the contribution of each colour component. Then the enhanced components are concatenated to generate the RGB colour image, which produces the gray image using PCA. The enhancement of each colour component using the CT and PCGF is carried out as follows.

Figure 2 Image enhancement results using the proposed method, (a) original colour image (b) red, green and blue channels (c) curvelet transform output (d) PCGF output (e) enhanced colour image (see online version for colours)

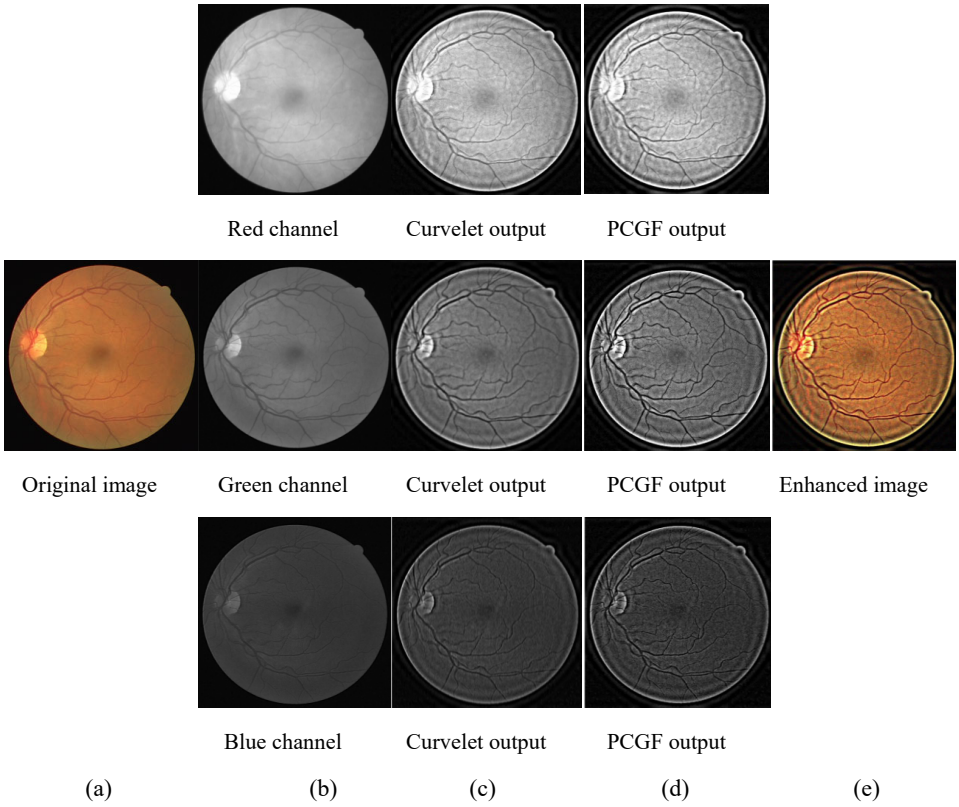

CT at level s and orientation θ, is applied to each colour component independently. It is to be noted here that the value of s and θ are experimentally determined and is discussed in the results section. The curvelet decomposition results in a set of curvelet coefficients for every level of decomposition at each orientation. The image is enhanced by modifying these coefficients so that high frequency curvatures and edges are emphasised while low frequency coarse regions are deemphasised. As discussed in Section 2.2, the coefficients at $s = 1$ corresponds to the coarse region and the coefficients for higher value of s corresponds to higher frequency regions. These coefficient modification strategies are unique and specific to the task at hand. In the proposed approach, the coefficient modification is done by setting all the coefficients for $s = 1$ to zero and multiplying a constant $\alpha (> 1)$ to the coefficients of all other levels. Then inverse CT is applied to the modified set of coefficients to reconstruct the image. Then the reconstructed image is subtracted from the corresponding colour component to get the enhanced image. Because the coefficient modification sets all coarse level coefficients to zero while raising fine level coefficients, the background in the reconstructed image appears darker while the curvatures and edges are highlighted. Several authors have proposed various ways for coefficient modification. Nevertheless, the suggested operation is very basic, straightforward, and effective. Furthermore, segmentation Acc is largely determined by the consistency of contrast throughout the image. The retinal image incorporates

non-uniform illumination that needed to be regulated before further processing. Although, CLAHE is popularly utilised for medical image enhancement but it fails to improve the image when the histogram of the original image is very narrow. The proposed approach involves red, green, and blue channels. Except the green channel other channels have very poor contrast. Hence, CLAHE is not preferred here. Therefore, we utilised the PCGF for contrast enhancement of the curvelet enhanced image. It takes both gamma and reciprocal of gamma values on the image and its complement to regulate the illumination variation. The gamma value in PCGF is experimentally selected and is discussed in the results section. The curvelet enhanced and PCGF corrected channels are then concatenated to get the enhanced colour image. Figure 2 illustrates the image enhancement outputs using the proposed CT and PCGF. Figure 2(a) shows the input colour image. The images in column 2(b) show the extracted colour components. Figures 2(c) and 2(d) show the curvelet enhanced and PCGF processed image respectively. Finally, Figure 2(e) shows the enhanced colour image formed by concatenating all the three colour components.

The enhanced colour image is annotated by using the conventional Coye algorithm. The enhanced colour image is converted to gray scale through PCA. This is done because the ground truth image available in both the databases is gray. An average filter of dimension 9×9 is utilised for the background elimination. Finally, ISODATA thresholding is applied to the background eliminated image to get the vessel network. Some minor disconnected vessel-like structures can be found in the ISODATA annotated result. The morphological opening operation is used for post-segmentation fine-tuning, which successfully removes the artefacts. It is important to mention here that the CLAHE stage for enhancement in the Coye algorithm is not used here because the input image is already enhanced using the proposed CT and PCGF.

The algorithm of the proposed method is given below:

Algorithm:

1. Read the RGB colour retinal image.
2. Separate the three colour channels of the input image.
3. For each colour channel do the enhancement:
    i. Apply curvelet decomposition and collect the coefficients.
    ii. Do the coefficient modification as:
        a) Set all the coefficients corresponding to $s = 1$ as *Zero*.
        b) Multiply α to all other coefficients.
    iii. Compute the reconstructed image using the modified set of coefficients.
    iv. Subtract the reconstructed image from the colour channel to obtain the curvelet enhanced colour channel.
    v. Apply PCGF to the above image to get the enhanced colour channel.
4. Concatenate the enhanced colour channels to get the colour enhanced image.
5. Abstract the gray image from the colour enhanced image through PCA.
6. Convolve the gray image with a mean filter of window size $W = 9 \times 9$.
7. Generate the difference image by subtracting the mean filtered image from the gray image.
8. Apply ISODATA for annotation of the above image.
9. Fine-tune the segmented result with morphological opening operation.

---

4 Results and discussion

The outcome of the proposed approach is evaluated on two freely available databases: DRIVE (Staal et al., 2004) and STARE (Hoover et al., 2000). The digital retinal images for vessel extraction (DRIVE) database has 40 colour retinal images arranged in two sets: Training set and Testing set. As the proposed approach is an unsupervised method so training set is not needed here. The testing set contains 20 colour fundus image, corresponding mask, and manually segmented vessel structure or ground truth. Each image has 24-bit gray scale resolution and 565×584 pixels' spatial resolution. The structured analysis of retina (STARE) dataset also has 20 colour retinal images of size 700×605. The manually labeled vessel structure for each image is also available in the dataset. The experiments are conducted on Intel core-i5 mainframe with 4GB RAM, running under Windows 10 operating system. The algorithms are implemented using MATLAB.

The segmented output of the suggested method is matched with the corresponding manually leveled image and true positive (TP), true negative (TN), false positive (FP), and false negative (FN) values are computed. TP denotes the count of the match of vessel pixels. TN denotes the count of the match of background pixels. FP is the count of background pixels incorrectly marked as the vessel in the segmented image. Similarly, FN is the count of vessel pixels incorrectly identified as background. Based on these counts, few statistical parameters are defined to measure the exactness of the segmented output. The effectiveness of the proposed method is quantified by three performance indices: Acc, Sensitivity, and Specificity. Acc shows the degree of matching of the segmented result with the manually leveled image. It is stated as below:

$$Acc = \frac{TP + TN}{TP + TN + FP + FN} \tag{6}$$

The sensitivity of an algorithm is its ability to find the vessel pixels cases correctly. Mathematically, it is defined as

$$Sensitivity = \frac{TP}{TP + FN} \tag{7}$$

Specificity is the quantity of non-vessel pixels which are precisely marked as itself.

$$Specificity = \frac{TN}{FP + TN} \tag{8}$$

Now to determine the curvelet decomposition level s and orientation θ a set of experiments are carried out by varying s from 1 to 6, and θ from 8 to 24. Each channel of the colour retinal image is decomposed by the CT and the coefficients are modified as per the proposed scheme. Here the value of α is chosen as 1.5. Then the curvelet enhanced image is segmented using the Coye algorithm and the average performance indices are computed. Tables 1 and 2 show the average performance indices obtained for various values of s and θ on the two datasets. It is witnessed from the tables that the highest Acc is achieved for s = 5, θ = 16 for DRIVE dataset and s = 6 and θ = 20 for the STARE dataset. Hence, we proceed with these set of parameters for the CT on the two datasets.

Table 1 Performance indices with parameter variation of CT for DRIVE database

CT Parameters	*Acc.*	*Sensitivity*	*Specificity*
s = 3, θ = 8	94.88	52.97	98.93
s = 4, θ = 8	94.74	54.48	98.63
s = 5, θ = 16	95.61	58.17	99.24
s = 5, θ = 20	95.60	58.09	99.14
s = 6, θ = 20	95.59	57.31	99.23
s = 6, θ = 24	95.49	57.29	99.13

Table 2 Performance indices with parameter variation of CT for STARE database

CT Parameters	*Acc.*	*Sensitivity*	*Specificity*
s = 3,θ = 8	94.96	57.17	98.02
s = 4, θ = 8	94.66	57.27	97.72
s = 5, θ = 16	95.37	62.62	97.88
s = 5, θ = 20	95.35	63.51	97.86
s = 6, θ = 20	95.63	64.12	98.35
s = 6, θ = 24	95.62	62.60	98.28

Another set of experiments is carried out to set the value of γ in the PCGF utilised in the proposed approach. The γ value is varied from 0.5 to 1.5 with an increment of 0.1 and the image segmentation is done as per the proposed scheme. The average Acc is computed. Figure 3 shows the average Acc for different values of γ. It is clear from the figure that $\gamma = 0.8$ gives the highest Acc for DRIVE database and $\gamma = 0.7$ is the best for the STARE database.

Figure 3 Variation of average accuracy with respect to γ (see online version for colours)

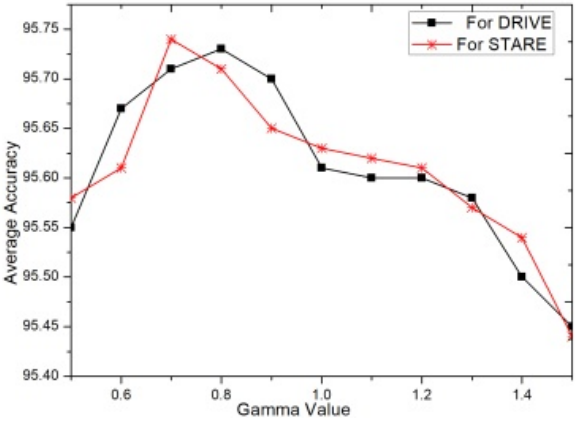

So the proposed approach proceeds with s = 5, θ = 16, and γ = 0.8 for DRIVE database and s = 6, θ = 20, and γ = 0.7 for STARE dataset. The output image at every stage of the proposed approach is displayed in Figures 4 and 5 for repository images of the two datasets. Figure 4(a) represents the original colour fundus image (Image 1) from DRIVE

dataset and Figure 4(b) represents the ground truth image. The enhanced colour image achieved by the proposed modification is shown in Figure 4(c). It clearly illustrates the intensification of the vessel lines. The gray image abstracted from it using PCA and the effect of contrast enhancement are shown in Figure 4(d). Figure 4(e) illustrates the background removed image. The ISODATA annotated image is displayed in Figure 4(f). A closer look at the annotated image shows that many falsely detected pixels appear with the vessel pixels. The post-processing approach efficiently removes these disconnected vessel pixels and the final segmented result is displayed in Figure 4(g) which closely matches the ground truth image.

Figure 4 Vessel segmentation results using drive dataset (a) original image (b) ground truth image (c) Enhanced image (d) Gray image obtained through PCA (e) background excluded image (f) ISODATA output (g) final segmented output (see online version for colours)

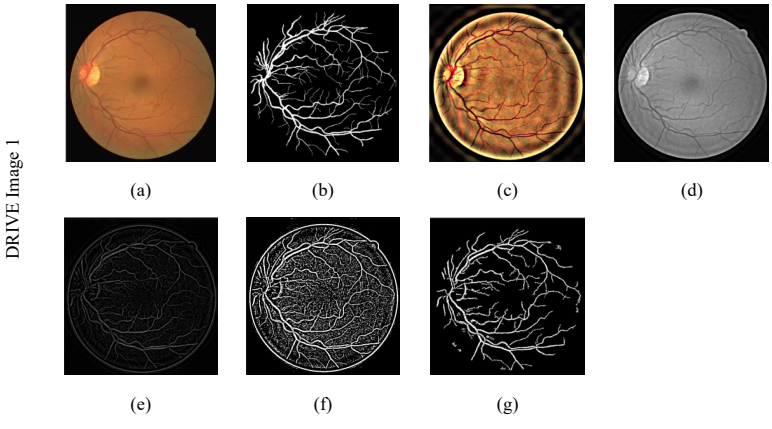

Similarly, Figure 5 represents the vessel segmentation results of colour fundus image (image 9) from STARE dataset.

Figure 5 Vessel segmentation results using stare dataset (a) original image (b) ground truth image (c) enhanced image (d) gray image obtained through PCA (e) Background excluded image, (f) ISODATA output, (g) final segmented output (see online version for colours)

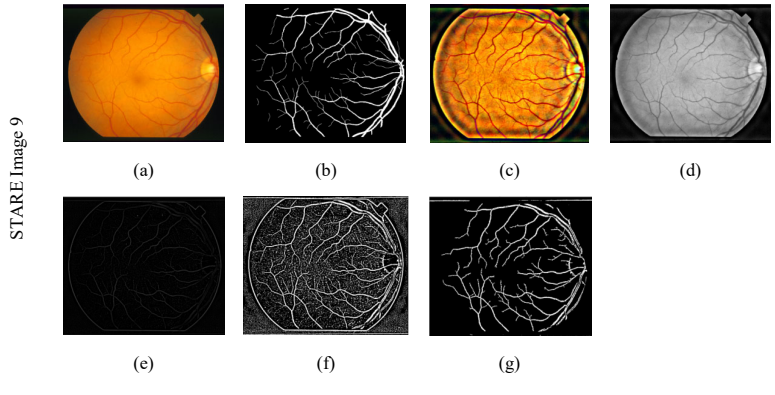

The performance indices computed for output images of the suggested approach are compared with Coye algorithm. The results are shown in Tables 4 and 5 for DRIVE and STARE datasets respectively. It can be inferred that the proposed method results in higher value of Acc for almost all the images. It is clearly observed that the proposed amendment to the Coye algorithm hiked the average Acc of segmentation to 95.73 for DRIVE dataset and to 95.75 for STARE dataset. There is also an increase in the value of sensitivity by around 3% for both these datasets. Also, the specificity is higher for the proposed approach as compared to the original Coye algorithm.

Table 4 Performance comparison using DRIVE database

Images	*Proposed*			*Coye*		
	Acc.	*Sensitivity*	*Specificity*	*Acc.*	*Sensitivity*	*Specificity*
Image 1	95.84	62.14	99.14	95.63	57.24	99.39
Image 2	95.22	57.12	99.57	94.83	51.17	99.81
Image 3	94.44	53.34	98.99	94.54	51.83	99.27
Image 4	95.54	56.75	99.47	95.20	50.31	99.75
Image 5	95.37	55.85	99.46	95.34	59.04	99.09
Image 6	95.88	51.11	99.60	94.41	44.18	99.82
Image 7	95.22	53.86	99.38	95.14	50.83	99.59
Image 8	95.85	52.90	98.80	87.42	65.39	89.50
Image 9	95.68	69.69	99.56	94.82	62.69	97.66
Image 10	95.86	59.13	99.16	95.57	63.52	98.44
Image 11	95.57	56.64	99.40	95.45	54.22	99.51
Image 12	95.68	59.42	99.11	95.59	64.83	98.49
Image 13	94.87	53.03	99.40	94.80	51.37	99.51
Image 14	96.02	62.05	99.01	95.88	54.56	99.51
Image 15	96.37	67.52	98.59	94.22	71.76	95.95
Image 16	95.93	59.43	99.55	95.30	49.90	99.80
Image 17	95.53	69.89	99.36	94.44	35.62	99.86
Image 18	96.31	68.08	99.17	96.05	56.45	99.46
Image 19	97.03	71.74	99.31	96.86	67.05	99.56
Image 20	96.39	63.67	98.99	88.54	77.65	89.40
Average	95.73	60.17	99.25	94.50	56.98	98.17

To further strengthen our claim, Figure 6 illustrates the comparison of the output images obtained using the original Coye algorithm and the proposed approach. A close observation of the images evidently states the superiority of the proposed approach as it draws the thin and fine vessels more efficiently. Moreover, the proposed method gives results close to the ground truth image. The reason may be due to the incorporation of the CT that provides very precise localisation of the curvatures and edges of vessels. The thin blood vessels have a very low contrast value and due to uneven illumination, these are almost meagre with the background. So the assimilation of PCGF in the proposed approach successfully neutralises the illumination variation and enhances the overall contrast of the image.

Table 5 Performance comparison using STARE database

Images	*Proposed*			*Coye*		
	Acc.	*Sensitivity*	*Specificity*	*Acc.*	*Sensitivity*	*Specificity*
Image 1	93.37	60.96	96.18	90.36	71.90	91.96
Image 2	94.10	54.32	96.94	91.22	66.36	92.99
Image 3	95.69	73.83	94.96	87.68	33.40	87.95
Image 4	94.93	67.66	99.51	94.34	56.26	97.39
Image 5	95.14	59.29	98.70	94.52	63.01	97.65
Image 6	95.98	74.99	97.55	91.12	81.95	91.81
Image 7	96.29	77.49	98.92	95.66	33.10	96.75
Image 8	96.24	73.76	98.05	96.28	77.90	97.76
Image 9	96.29	73.33	98.24	96.00	79.87	97.38
Image 10	94.96	68.32	98.29	93.50	76.28	95.00
Image 11	97.06	70.48	99.10	96.70	77.26	98.19
Image 12	97.27	76.21	99.03	96.96	79.23	98.44
Image 13	95.86	69.78	98.41	94.48	38.67	96.02
Image 14	95.80	67.87	98.58	94.25	77.41	95.93
Image 15	95.48	61.07	98.73	94.92	70.72	97.20
Image 16	94.39	55.85	98.77	94.13	55.49	98.52
Image 17	96.22	69.07	98.89	96.00	70.91	98.46
Image 18	97.36	54.35	99.65	96.17	64.53	97.85
Image 19	97.15	52.55	99.55	95.74	39.24	99.64
Image 20	95.34	65.90	98.88	94.22	60.88	96.60
Average	*95.75*	*66.35*	*98.35*	94.21	63.72	96.18

Figure 6 Segmentation results (a) original images (b) ground truth images (c) Coye algorithm outputs (d) proposed approach outputs

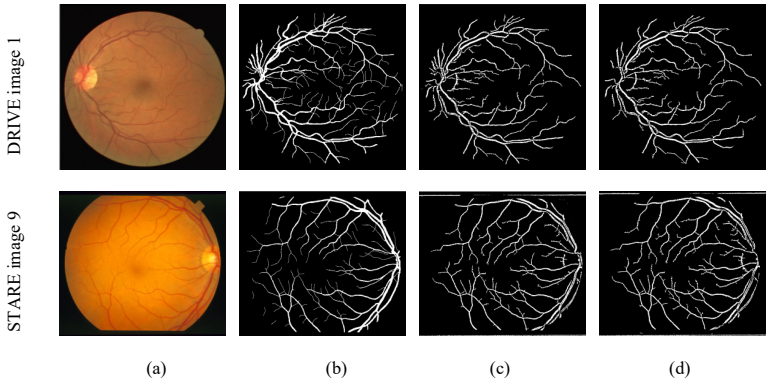

A bar graph representing the effect of the modification to the original Coye algorithm is also presented in Figure 7 for easy interpretation. The higher value of sensitivity and specificity indicates that both the vessel and non-vessel pixels are classified more

accurately. The proposed method outperforms the original Coye algorithm for both the different databases with versatile images. Hence, it can be asserted that the suggested modification leads to a more efficient and robust method.

Figure 7 Graphical comparison of the average values of the performance indices for Coye algorithm and the proposed approach (a) drive dataset (b) stare dataset (see online version for colours)

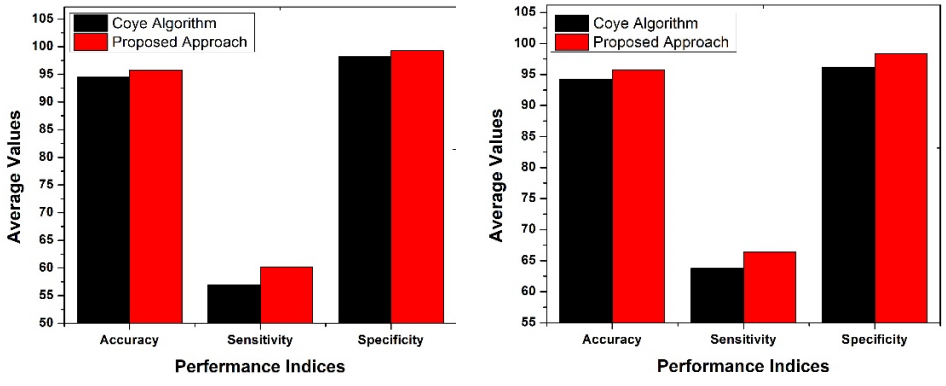

(a) (b)

The performance of the suggested approach is also compared with a few of the existing methodologies. Table 6 and Table 7 show the comparison in terms of Acc, sensitivity, and specificity with the state-of-the-art approaches for DRIVE and STARE databases respectively.

Table 6 Performance comparison with state-of-the-art methods using DRIVE dataset

Methods	*Acc.*	*Sensitivity*	*Specificity*
Strisciuglio et al. (2016)	94.54	77.77	97.02
Zhou et al. (2020)	94.75	72.62	98.03
Pal et al. (2019)	94.31	61.29	97.44
Khan et al.(2019a)	94.40	75.40	96.40
Bandara and Giragama (2017)	94.11	74.32	96.66
Miri and Mahloojifar (2010)	94.52	73.44	97.64
Mapayi et al. (2015)	94.61	76.32	96.34
Soares et al. (2006)	94.66	-	-
Sreejini and Govindan (2015)	95.00	71.72	96.87
Roychowdhury et al. (2015)	95.20	72.50	98.30
Dash et al. (2020)	95.20	75.60	98.10
Wang et al. (2013)	94.61	-	-
Dash and Bhoi (2017)	95.50	71.90	-
Original Tyler Coye algorithm	94.50	56.98	98.17
Proposed approach	95.73	60.17	99.25

Table 7 Performance comparison with state-of-the-art methods on STARE dataset

Methods	*Acc.*	*Sensitivity*	*Specificity*
Strisciuglio et al. (2016)	95.34	80.46	97.10
Khan et al. (2019b)	94.80	75.20	95.60
Bandara and Giragama (2017)	94.89	78.85	96.76
Zhou et al. (2020)	95.30	77.54	97.39
Mapayi et al. (2015)	95.10	76.26	96.57
Soares et al. (2006)	94.80	-	-
Roychowdhury et al. (2015)	95.10	77.20	97.30
Wang et al. (2013)	95.21	-	-
Original Tyler Coye algorithm	94.21	63.72	96.18
Proposed approach	95.75	66.33	98.35

Note: '-' indicates non availability of data.

From both the tables, it is observed that, the suggested strategy achieves the highest average Acc and specificity for both the database while maintaining comparable sensitivity values. For instance, Bandara and Giragama (2017) used the Tyler Coye variation that was modified with a Hough line transformation, but it achieved an average Acc of 94.11 for DRIVE and 94.89 for STARE. Miri and Mahloojifar (2011) implemented curvelet based retinal image enhancement with a non-linear coefficient modification strategy. However, they ended up with an average Acc of 94.52 on DRIVE images. The specificity value is below 99 for all these methods on DRIVE dataset. Conversely, the proposed approach achieves a specificity value of 99.25. The sensitivity value of the proposed approach is a bit lower. The reason may be the optic disk interference that needs to be removed before vessel annotation. The execution time of the suggested approach is also very less, i.e., around 3.11 secs as compared to 8.3 secs in Roychowdhury et al. (2015), and 10 secs in Strisciuglio et al. (2016).

5 Conclusions

This paper presents an automatic method of blood vessel extraction from fundus images by uniting curvelet decomposition and PCGF with Tyler Coye algorithm. As the vessels are curvilinear structures so CT can be best suited for highlighting the vessel edges, curvatures, and boundaries. As the proposed approach considers all the three channels of colour retinal image, the PCGF is demonstrated to be a better suitable for enhancement of low, high and moderate contrast images. The integration of curvelet decomposition and PCGF strongly intensify both the thick and the thin vessels. Hence, it delivers better segmentation performance. The average segmentation Acc, sensitivity, and specificity are 94.50, 56.98, and 98.17 respectively for Coye algorithm using the DRIVE dataset. This has improved to 95.73, 60.17 and 99.25 respectively using the proposed approach. Similarly, the Acc, sensitivity, and specificity values also get enhanced from 94.21, 63.72 and 96.18 to 95.75, 66.33 and 98.35 respectively in case of STARE dataset. The achieved results confirm that the developed algorithm can be reliably implemented for automatic extraction of blood vessels in the fundus image. The proposed technique has a slightly lower sensitivity value. It's possible that the cause is interference with the optic disc,

which needs to be removed before vessel annotation. Even though the segmentation results are promising, they can further be enhanced by considering the optimum set of parameters for CT and PCGF. In future, the sensitivity and the Acc values can be improved by assimilating deep learning based classifiers.

References

Bandara, A.M.R.R. and Giragama, P.W.G.R.M.P.B. (2017) 'A retinal image enhancement technique for blood vessel segmentation algorithm', In *2017 IEEE International Conference on Industrial and Information Systems* (ICIIS), IEEE, pp.1–5.

Coye, T. (2015) *A Novel Retinal Blood Vessel Segmentation Algorithm for Fundus Images*, MATLAB Central File Exchange [online] http://www.mathworks.com/matlabcentral/fileexchange/50839 (accessed June 2020).

Dash, J. and Bhoi, N. (2017) 'A thresholding based technique to extract retinal blood vessels from fundus images', *Future Computing and Informatics Journal*, Vol. 2 No. 2, pp.103–109.

Dash, J., Priyadarsan, P. and Nilamani, B. (2020) 'Retinal blood vessel extraction from fundus images using enhancement filtering and clustering', *ELCVIA: Electronic Letters on Computer Vision and Image Analysis*, Vol. 19, No. 1, pp.38–52.

Dash, S. and Senapati, M.R. (2020) 'Enhancing detection of retinal blood vessels by combined approach of DWT, Tyler Coye and Gamma correction', *Biomedical Signal Processing and Control*, Vol. 57, pp.101740.

Donoho, D.L. and Duncan, M.R. (2000) 'Digital curvelet transform: strategy, implementation, and experiments', *Wavelet applications, International Society for Optics and Photonics*, Vol. 4056, pp.12–30.

Gonzalez, R.C., Woods, R.E. and Eddins, S.L. (2004) *Digital Image Processing*, Pearson Education India, Chennai, Tamil Nadu.

Hoover, A., Kouznetsova, V. and Goldbaum, M. (2000) 'Locating blood vessels in retinal images by piece-wise threhsold probing of a matched filter response', *IEEE Transactions on Medical Imaging*, Vol. 19, No. 3, pp.203–210.

Kar, S.S. and Maity, S.P. (2016) 'Blood vessel extraction and optic disc removal using curvelet transform and kernel fuzzy c-means', *Computers in Biology and Medicine*, Vol. 70, pp.174–189.

Khan, K.B., Khaliq, A.A., Jalil, A., Iftikhar, M.A., Ullah, N., Aziz, M.W. and Shahid, M. (2019) 'A review of retinal blood vessels extraction techniques: challenges, taxonomy, and future trends', *Pattern Analysis and Applications*, Vol. 22, No. 3, pp.767–802.

Khan, M.A., Khan, T.M., Soomro, T.A., Mir, N. and Gao, J. (2019) 'Boosting sensitivity of a retinal vessel segmentation algorithm', *Pattern Analysis and Applications*, Vol. 22, No. 2, pp.583–599.

Koh, J.E.W. et al. (2017) 'Diagnosis of retinal health in digital fundus images using continuous wavelet transform (CWT) and entropies', *Computers in Biology and Medicine*, Vol. 84, pp.89–97.

Li, C. et al. (2020) 'Low-light image enhancement via pair of complementary gamma functions by fusion', *IEEE Access*, Vol. 8, pp.169887–169896.

Mapayi, T., Viriri, S. and Tapamo, J-R. (2015) 'Adaptive thresholding technique for retinal vessel segmentation based on GLCM-energy information', *Computational and Mathematical Methods in Medicine*, Vol. 2015, pp.1–11.

Memari, N., Saripan, M.I.B., Mashohor, S. and Moghbel, M. (2019) 'Retinal blood vessel segmentation by using matched filtering and fuzzy c-means clustering with integrated level set method for diabetic retinopathy assessment', *Journal of Medical and Biological Engineering,* Vol. 39, No. 5, pp.713–731.

Miri, M.S. and Mahloojifar, A. (2010) 'Retinal image analysis using curvelet transform and multistructure elements morphology by reconstruction', *IEEE Transactions on Biomedical Engineering*, Vol. 58, No. 5, pp.1183–1192.

Moccia, S. et al. (2018) 'Blood vessel segmentation algorithms–review of methods, datasets and evaluation metrics', *Computer Methods and Programs in Biomedicine*, Vol. 158, pp.71–91.

Pal, S., Chatterjee, S., Dey, D. and Munshi, S. (2019) 'Morphological operations with iterative rotation of structuring elements for segmentation of retinal vessel structures', *Multidimensional Systems and Signal Processing*, Vol. 30, No. 1, pp.373–389.

Reddy, P.S. et al. (2018) 'Retinal fundus image enhancement using piecewise gamma corrected dominant orientation based histogram equalization', *International Conference on Communication and Signal Processing* (ICCSP), IEEE, pp.124–128.

Ricci, E. and Perfetti, R. (2007) 'Retinal blood vessel segmentation using line operators and support vector classification', *IEEE Transactions on Medical Imaging*, Vol. 26, No. 10, pp.1357–1365.

Roychowdhury, S., Koozekanani, D.D. and Parhi, K.K. (2014) 'Blood vessel segmentation of fundus images by major vessel extraction and subimage classification', *IEEE Journal of Biomedical and Health Informatics*, Vol. 19, No. 3, pp.1118–1128.

Soares, J.V.B. et al. (2006) 'Retinal vessel segmentation using the 2-D Gabor wavelet and supervised classification', *IEEE Transactions on Medical Imaging*, Vol. 25, No. 9, pp.1214–1222.

Sreejini, K.S. and Govindan, V.K. (2015) 'Improved multiscale matched filter for retina vessel segmentation using PSO algorithm', *Egyptian Informatics Journal*, Vol. 16, No. 3, pp.253–260.

Staal, J., Abràmoff, M.D., Niemeijer, M., Viergever, M.A. and Van Ginneken, B. (2004) 'Ridge-based vessel segmentation in color images of the retina', *IEEE Transactions on Medical Imaging*, Vol. 23, No. 4, pp.501–509.

Starck, J-L. et al. (2003) 'Gray and color image contrast enhancement by the curvelet transform', *IEEE Transactions on Image Processing*, Vol. 12, No. 6, pp.706–717.

Strisciuglio, N. et al. (2016) 'Supervised vessel delineation in retinal fundus images with the automatic selection of B-COSFIRE filters', *Machine Vision and Applications*, Vol. 27, No. 8, pp.1137–1149.

Wang, Y. et al. (2013) 'Retinal vessel segmentation using multiwavelet kernels and multiscale hierarchical decomposition', *Pattern Recognition*, Vol. 46, No. 8, pp.2117–2133.

Yadav, N. (2020) 'Retinal blood vessels detection for diabetic retinopathy with Ridgelet transform and convolution neural network', *International Journal of Wavelets, Multiresolution and Information Processing*, Vol. 18, No. 6, p.2050048.

Zhou, C., Zhang, X. and Chen, H. (2020) 'A new robust method for blood vessel segmentation in retinal fundus images based on weighted line detector and hidden Markov model', *Computer Methods and Programs in Biomedicine*, Vol. 187, p.105231.